ISSN 0036-0244, Russian Journal of Physical Chemistry A, 2022, Vol. 96, No. 12, pp. 2747–2756. © Pleiades Publishing, Ltd., 2022.

PHYSICAL CHEMISTRY OF SEPARATION PROCESSES. CHROMATOGRAPHY

Heterogeneous Epoxidation of α-Pinene with Air over Mordenite (MOR) Supported Cobalt Complex

Xixi Li[a], Xinhuan Lu[a,*], Run Jing[a], Haifu Zhang[a], Chenlong Wang[a], Huaxin Zhang[b], Beibei Wang[a], Dan Zhou[a], and Qinghua Xia[a,]**

[a] *Collaborative Innovation Center for Advanced Organic Chemical Materials Co-constructed by the Province and Ministry, Ministry-of-Education Key Laboratory for the Synthesis and Application of Organic Functional Molecules, Ministry-of-Education Key Laboratory for Green Preparation and Application of Functional Materials, Hubei University, Wuhan, 430062 China*

[b] *Jingchu University of Technology, Jingmen, 448000 China*

** e-mail: xinhuan003@aliyun.com*

*** e-mail: xiaqh518@aliyun.com*

Received October 15, 2021; revised October 15, 2021; accepted October 30, 2021

Abstract—The MOR supported cobalt complex materials were synthesized by ion exchange method and used to catalyze the epoxidation reaction of α-pinene with air. The liquid phase batch mode of epoxidation reaction was carried out under atmospheric pressure and aerobic conditions. Among the supported $[Co(NH_3)_6]^{3+}$-zeolites catalysts, $[Co(NH_3)_6]^{3+}$-MOR exhibited the best catalytic efficiency for the titled reaction, and high reaction conversion as well as epoxidation product selectivity were obtained for α-pinene and α-epoxypinane. Parametric studies were performed to examine the effect factors like the Co content, the solvent, the initiator, the substrate amount and the catalyst amount. The catalyst can be reused at least nine cycles without significant loss in activity towards epoxidation.

Keywords: cobalt complex, MOR supported, olefin, epoxidation, air

DOI: 10.1134/S0036024422120317

INTRODUCTION

The catalytic oxidation reaction of alkenes played an important role in catalytic reaction, since their epoxy products were crucial building blocks in organic synthesis, which was widely used in the preparation of biological materials, pharmaceuticals, fine chemical and polymers as intermediates [1–7], e.g., propylene oxide was extensively used in the industrial production, and its annual output exceeded 10 million tons in 2009 [8]. Epoxy styrene could be used as pharmaceutical intermediates, dyes, perfumes and resin additives [9, 10]. Therefore, the research and development of olefin epoxidation reaction was of great academic and industrial importance.

During the last decade, in consideration of the concept of environmental friendliness and economy, numerous efforts have concentrated on the seeking for efficient catalyst [11–13]. Polyoxometalate (POMs) nanoclusters could be directly used as high-efficiency catalysts in epoxidation. Liu et al. reported the epoxidation reaction of allyl alcohols and aqueous H_2O_2 catalyzed by self-assembled $[WZn_3(ZnW_9O_{34})_2]^{12-}$ catalyst [14]. Under surface reaction conditions, Jameel et al. employed chloropropyltriethoxysilane-functionalized SBA-15 as a carrier to immobilize $Na_9PMo_{11}O_{39}$ (PMo_{11}) and aurum nanoparticles [15]. In recent years, nanocatalysts have been studied as alternatives to conventional catalysts. Wang et al. reported a simple and effective method for synthesizing Ag/SBA-15 nanostructures, which could be applied to styrene epoxy with 63.7% conversion and 79.6% selectivity [16]. Some nanostructured catalysts, such as Co_3O_4, Fe_2O_3, and mixed Fe–Co oxides have been applied to the hydrocarbon oxidations [17, 18].

In recent years, the wide applications of molecular sieve materials in the epoxidation of olefins have attracted more and more attention. The excellent catalytic performance for olefins was due to high surface area, big pore size, excellent mechanical and thermal stability. During the past decade, numerous researchers have paid attention to silico-aluminophosphate molecular sieve SAPO which had outstanding catalytic performance for a series of reactions [19–21]. In 2004, Tang et al. [22, 23] first reported that in the absence of co-reducing agent, using molecular oxygen as an oxidant, the Co^{2+}-exchanged zeolite catalysts can effectively catalyze the epoxidation of styrene. Luts et al. attached Mo(IV)–Salen complexes covalently to silica supports and then researched their

epoxidation properties, which made it easy to separation and recovery and improved their performance and commercial value [24]. Bakala et al. inserted highly dispersed molybdenum oxide species into SBA-15, MCM-41, and other silica material, which was used for liquid phase epoxidation of olefins with H_2O_2 oxidant [25].

Due to its low cost and environmental friendliness, selective oxidation of olefin with O_2 has been more attractive and challenging [26]. Catalytic epoxidation using molecular oxygen as an oxygen source under mild conditions have been a huge challenge for researchers [2, 27], in which our group has been published some works [28–34]. In this work, the trivalent cobalt-ammonia complex $[Co(NH_3)_6]Cl_3$ was supported onto the molecular sieve. The characterization results showed that the molecular sieve skeleton remained intact, the cobalt-ammonia complex was uniformly and highly dispersed on the surface. 3%$[Co(NH_3)_6]^{3+}$-MOR showed the highest catalytic activity and excellent recycle stability.

EXPERIMENTAL

Materials

The molecular sieves such as Na-ZSM-5, Na-Y, etc. were bought from Nankai Co. Ltd. $Co(Ac)_2{\cdot}4H_2O$, $CoCl_2{\cdot}6H_2O$, $Co(NO_3)_2{\cdot}H_2O$ and all alkenes such as α-pinene, styrene, etc. were bought from Aladdin Industrial Corporation. THF (tetrahydrofuran), CHP (cumene hydroperoxide), DMF (*N*,*N*-dimethylformamide), DMA (*N*,*N*-dimethylacetamide), and metal salts were purchased from China National Medicines Corporation Ltd. The primary reagents such as olefins, reaction solvents and oxidants were used directly without further purification.

Synthesis of Cobalt(III) Ammonia Complex

$[Co(NH_3)_6]Cl_3$ (hexaamminecobalt(III) chloride) was synthesized by the method of Bjerrum and McReynold [35]: An appropriate quantity of $CoCl_2{\cdot}6H_2O$ (6.0 g, 25.2 mmol) was poured into a 100 mL conical flask containing the mixture of 4.0 g NH_4Cl (74.8 mmol) and 8.4 g deionized water under stirring, followed by the addition of 0.4 g coconut shell charcoal. After the solution was cooled down, 12.5 mL ammonium hydroxide was instilled into the above solution with stirring. The flask was covered until the solution was cooled down to 0°C. Subsequently, 13.5 mL 5% H_2O_2 was added into the flask, and then the resulting liquid was heated in water bath at 50–60°C for 35 min while stirring. After the liquid was cooled down again, the black solid was recovered by filtration, and then dissolved into 60 mL boiling water contained 1.7 mL concentrated hydrochloric acid. After rapid filtration, 6.7 mL of concentrated hydrochloric acid was slowly added to the solution and cooled down. The coarse product was recovered by filtration.

Synthesis of x%$[Co(NH_3)_6]^{3+}$-MOR

An appropriate quantity of $[Co(NH_3)_6]Cl_3$ and 1 g Na-MOR molecular sieve were added to a round bottom flask containing 50 g deionized water. The liquid was ion-exchange at 80°C for 10 h while stirring. The solid was obtained by filtration, then repeatedly washed with deionized water and dried to obtain the catalyst. The sample synthesized under ion-exchange method was named as *x*%$[Co(NH_3)_6]^{3+}$-MOR. Similarly, the catalyst prepared by impregnation method was named 10%$[Co(NH_3)_6]^{3+}$/MOR.

Characterizations of Materials

The phase analysis was carried out using the German Bruker D8A25 XRD diffractometer. The test conditions were as follows: Cu target K_α: λ = 1.54184 Å as the radiation source, voltage 40 kV, current 40 mA, scan range 2θ = 5°–80°. Scanning electron microscope JEOL JSM-6510A was used to detect the morphology and size of the catalyst. The sample structure was tested by the US FEI Tecnai G20 transmission electron microscope, and the test voltage was 200 kV. Perkin Elmer Spectrometers and attenuation total reflection (ATR) were used to record IR spectra of solid samples at the range of 2000–400 cm^{-1}. UV–Vis spectra of catalysts were investigated on a TU-1901 spectrometer at the range of 200–500 nm.

Catalytic Epoxidation of Olefin

Typically, the epoxidation reaction was conducted in a 50 mL two-necked round-bottom glass flask, the reaction process comprised following steps: 3 mmol of α-pinene, 30 mg of catalyst, 0.3 mmol of CHP, and 10 g of DMF were put into the flask. After being heated to 90°C, the air was added into the solution at the rate of 40 mL/min while stirring vigorously by a magnetic stirrer. The epoxidation process lasted 5 h and the catalyst was centrifuged. After that, the solid catalyst was washed with ethanol, followed by drying in an oven at 80°C for 12 h. The reaction solution was analyzed by GC-9720 that equipped with an FID detector.

RESULTS AND DISCUSSION

Structure Description

$[Co(NH_3)_6]Cl_3$ was synthesized by ion exchange method (Scheme 1). The XRD patterns of MOR, $[Co(NH_3)_6]Cl_3$ and $[Co(NH_3)_6]^{3+}$-MOR were shown in Fig. 1, which indicated the intact framework structures of MOR after ion-exchange treatment (2θ = 6.5°, 8.6°, 9.76°, 13.44°, 13.82°, 22.18°, 25.60°,

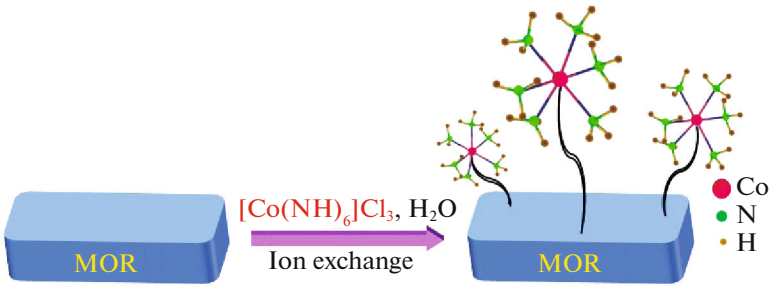

Scheme 1. Schematic illustration for the preparation of $x\%[Co(NH_3)_6]^{3+}$-MOR.

27.66°). The disappearance of the diffraction peak of $[Co(NH_3)_6]Cl_3$ indicated that the trivalent cobalt-ammonia complex has been highly dispersed onto the surface of the porous support. The XRD spectra of the other zeolites supported $[Co(NH_3)_6]Cl_3$ materials were shown in Fig. S1 (see Supplementary Material). Similar to the material of $[Co(NH_3)_6]^{3+}$-MOR, the framework structure of various zeolites remained intact after ion-exchange treatment. Due to the high dispersion of $[Co(NH_3)_6]^{3+}$ ions on these zeolites, almost no diffraction peaks of $[Co(NH_3)_6]Cl_3$ were observed. The XRD spectra of $x\%[Co(NH_3)_6]^{3+}$-MOR materials have been shown in Fig. S2. As the cobalt loading increased, the diffraction peak intensity of MOR did not change significantly, indicating that the content of cobalt exchange had no effect on the structure of zeolite.

The IR spectra of $[Co(NH_3)_6]^{3+}$-MOR and the precursor materials were shown in Fig. 2. We knew that the absorption peak at 1041 cm^{-1} belonged to Si–O–Si tetrahedral asymmetrical tensile stretching vibration, while the characteristic absorption peak at 452 cm^{-1} belonged to Si–O bond bending vibration. The infrared spectra of the molecular sieve MOR and the catalyst $[Co(NH_3)_6]^{3+}$-MOR showed that the structure of MOR was unchanged after loading with $[Co(NH_3)_6]Cl_3$, which consistent with the XRD results. The characteristic absorption peak of $[Co(NH_3)_6]Cl_3$ was not observed in the infrared spectra, which might be due to its high dispersion. Fourier-transform infrared (FTIR) spectra of zeolites and $[Co(NH_3)_6]^{3+}$-zeolite were illustrated in Fig. S3. Similar to $[Co(NH_3)_6]^{3+}$-MOR, the characteristic absorption peak of other zeolites also remained unchanged. The UV–Vis spectra of MOR and $[Co(NH_3)_6]^{3+}$-MOR have been shown in Fig. S4, which indicated that the curve of MOR showed no absorption peaks at 350–500 nm. As can be seen from the curve of $[Co(NH_3)_6]^{3+}$-MOR, it exhibited a broad absorption band at 390 nm while $[Co(NH_3)_6]^{3+}$ had characteristic absorption at 370 and 550 nm.

The difference between the surface morphology of MOR and $[Co(NH_3)_6]^{3+}$-MOR materials can be

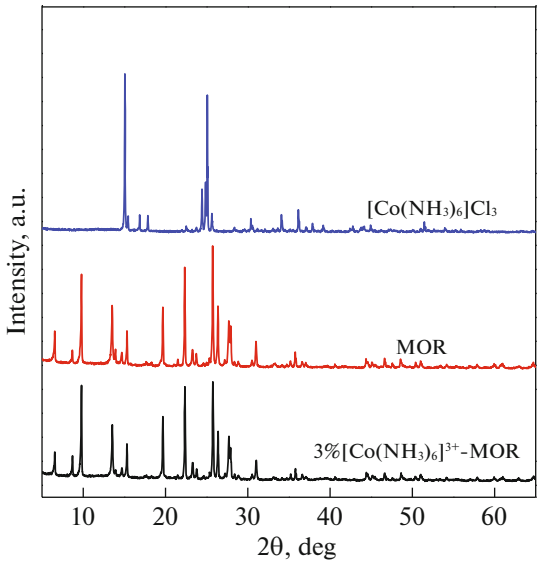

Fig. 1. XRD patterns of materials.

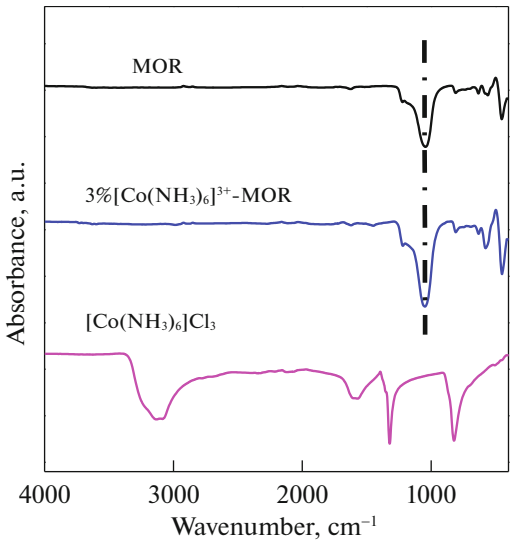

Fig. 2. IR spectra of materials.

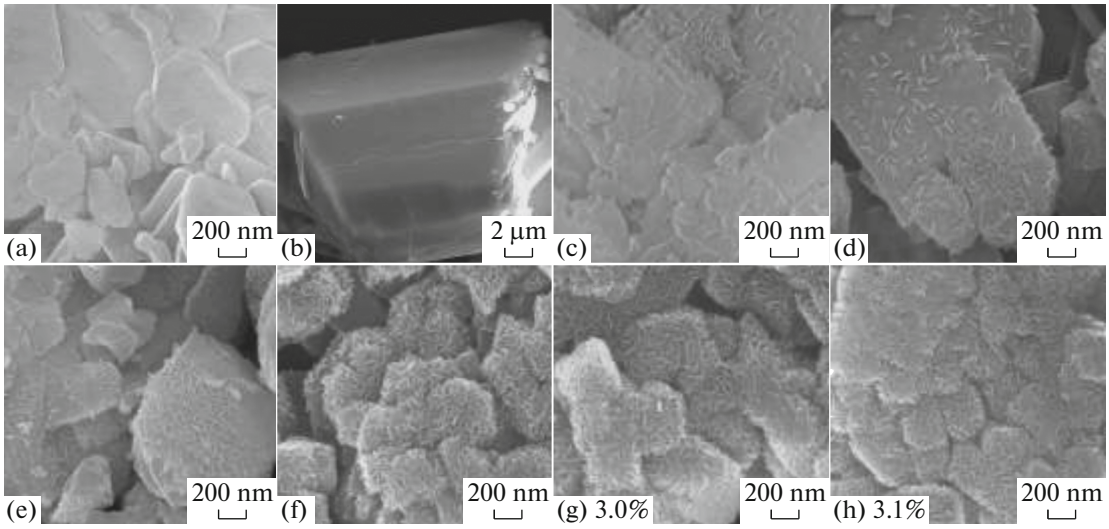

Fig. 3. SEM images of MOR (a), $[Co(NH_3)_6]Cl_3$ (b), and $x\%[Co(NH_3)_6]^{3+}$-MOR (c–h).

clearly obtained in Fig. 3. From Fig. 3a, it can be seen that the MOR was typical layer-stack structure, and its surface was relatively smooth. The $[Co(NH_3)_6]Cl_3$ showed a micron-level columnar morphology with a large grain size. As could be seen clearly from the diagram, MOR was obviously encapsulated by $[Co(NH_3)_6]^{3+}$ acicular crystals with the increase of $[Co(NH_3)_6]Cl_3$. When only 0.8%$[Co(NH_3)_6]Cl_3$ and 1.5%$[Co(NH_3)_6]Cl_3$ were added, the naked MOR (Figs. 3c and 3d) could be clearly seen. With the increase of $[Co(NH_3)_6]Cl_3$ addition, the shell thickness of $[Co(NH_3)_6]^{3+}$ gradually increased (Figs. 3e–3h). When the addition of $[Co(NH_3)_6]Cl_3$ increased to 2.8–3.1% (7–15% theoretical exchange volume, actual Co content of 2.8–3.1%), MOR was wrapped by a very thick $[Co(NH_3)_6]^{3+}$ shell. According to the activity test results of the corresponding catalysts, we knew that when the exchange amount of $[Co(NH_3)_6]Cl_3$ was larger than 2.2%, the amount of $[Co(NH_3)_6]^{3+}$ acicular crystal was correspondingly larger, so the active sites of the catalyst were greatly increased, which led to the enhanced catalytic activity. The TEM images further characterized the surface morphology of the materials. As can be seen from Fig. 4, acicular crystals were uniformly stacked on the surface of MOR, and the length and width were about 50–100 nm and a few nanometers, respectively, indicating that $[Co(NH_3)_6]^{3+}$ was uniformly exchanged and highly dispersed on the surface of MOR.

The XPS spectra of Co 2*p* core level of the $[Co(NH_3)_6]^{3+}$-MOR was investigated in Fig. 5. The peak of 780.5 eV belonged to Co $2p_{2/3}$, which attributed to the shift of Co $2p_{2/3}$ (781.6 eV) of $[Co(NH_3)_6]Cl_3$. The XPS measurement confirmed that $[Co(NH_3)_6]^{3+}$ remained trivalent after ion exchange. Figure 6 showed the TG curves of MOR, $[Co(NH_3)_6]Cl_3$ and $[Co(NH_3)_6]^{3+}$-MOR materials. Evidently, the TG curve of $[Co(NH_3)_6]Cl_3$ showed a weight loss range at 230–700°C (~74.0%). As can be seen from the TG curves of MOR and $[Co(NH_3)_6]^{3+}$-MOR, the weight loss below 250°C attributed to physical adsorption and evaporation of bound water in the molecular sieve framework, then MOR had almost no weight loss (~1.2%), but the weight loss of 3%$[Co(NH_3)_6]^{3+}$-MOR continued to ~700°C, indicating that the weight loss in the range of 250–700°C was due to the cobalt ammonium ion (~6.4%).

Catalytic Activity of the Supported Catalysts

The catalytic activity of different molecular sieves supported $[Co(NH_3)_6]Cl_3$ catalysts was concluded in Table 1. When only Na-MOR catalyst was used (Entry 1), the conversion of α-pinene was only 2.9%, and the activity was extremely lower than that of the other catalysts. When ion-exchanged $[Co(NH_3)_6]^{3+}$-MOR was used (Entry 2), the conversion of olefin (α-pinene) achieved 97.8%, and the selectivity of α-epoxypinane was 95.2%. Compared with $[Co(NH_3)_6]Cl_3$, the content of active metal Co in $[Co(NH_3)_6]^{3+}$-MOR was 3.0%, and the TON value was the highest of 192.0. Entries 3–7 showed the impact under the same conditions of other molecular sieves exchanged $[Co(NH_3)_6]^{3+}$ catalysts. It was revealed that the catalyst obtained by Y and β exchange could achieve the conversion >89% with >86% selectivity of epoxide, which showed an excellent catalyst activity. Using the catalyst obtained by ZSM-5 exchange, the conversion of α-pinene and selectivity of epoxide could achieve 77.7 and 90.6%. Similarly, the catalytic activity of $[Co(NH_3)_6]^{3+}$-13X

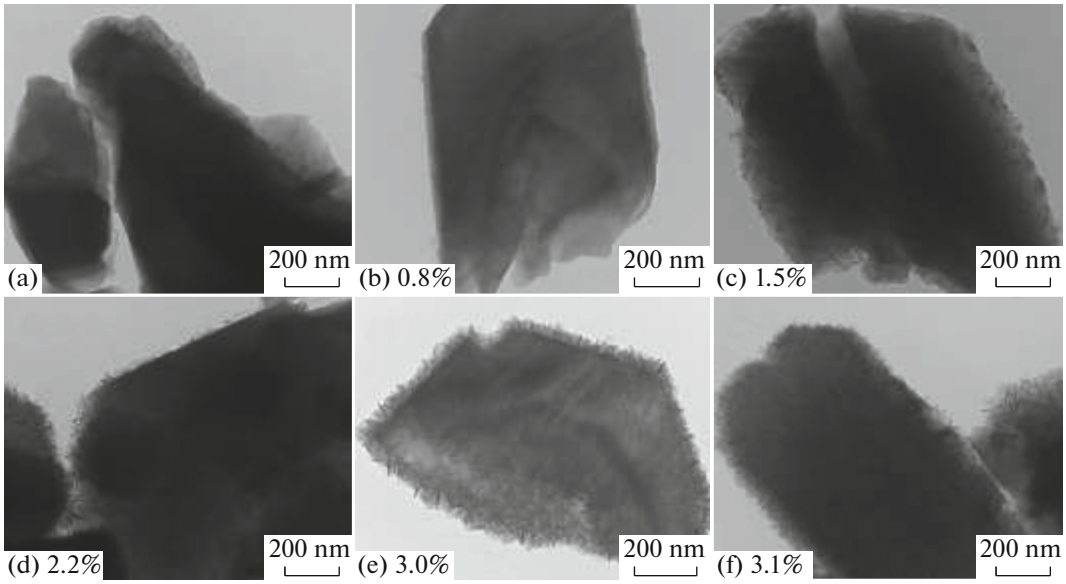

Fig. 4. TEM images of MOR (a) and $x\%[Co(NH_3)_6]^{3+}$-MOR (b–f).

was also lower than $[Co(NH_3)_6]^{3+}$-MOR and the conversion of α-pinene was 71.2%. The catalyst obtained by MCM-22 exchange had α-pinene conversion of 84.5%, but the selectivity of α-epoxydecane was merely 78.8%. When $10\%[Co(NH_3)_6]Cl_3$/MOR synthesized by the impregnation method was added (Entry 8), the conversion of α-pinene was 85.5%, and correspondingly the TON value was only 15.1, which was equivalent to the TOF value (14.8) of $10\%[Co(NH_3)_6]Cl_3/SiO_2$ synthesized by the same impregnation method (Entry 9). While TiO_2 was used as the carrier, $10\%[Co(NH_3)_6]Cl_3/TiO_2$ merely converted 31.1% of α-pinene with only 5.5 of the TON value.

For purpose of studying the impact of the Co content on the epoxidation of α-pinene, a series of $[Co(NH_3)_6]^{3+}$-MOR catalysts with different content of $[Co(NH_3)_6]Cl_3$ was prepared and applied in the titled reaction (Fig. 7). When only MOR was added, the catalytic activity was very poor with only 2.9% α-pinene conversion. While only a small amount of cobalt ($0.8\%[Co(NH_3)_6]^{3+}$-MOR, 1% theoretical exchange volume, actual Co content of 0.8%) was used, the α-pinene conversion and the epoxide selectivity were dramatically improved (49.4 or 94.4%, respectively), which demonstrated that cobalt was an important active center in this system. As the cobalt content increased (3–10% theoretical exchange vol-

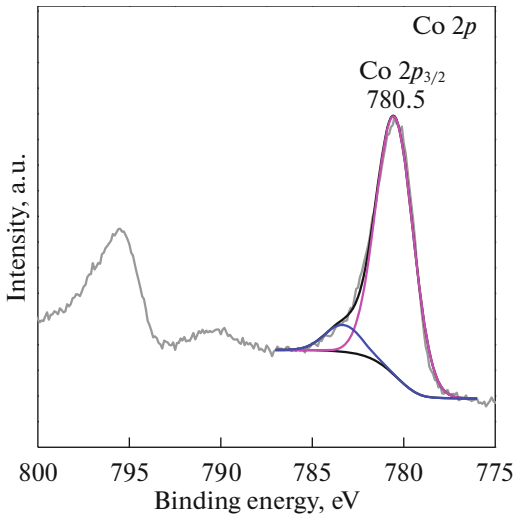

Fig. 5. XPS spectra of $3\%[Co(NH_3)_6]^{3+}$-MOR.

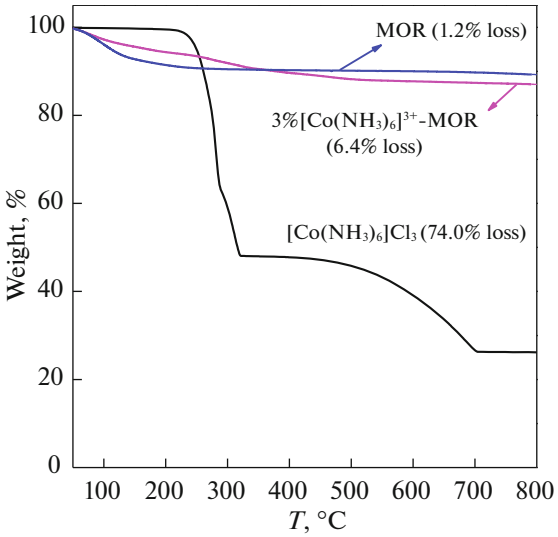

Fig. 6. TG curves of materials.

Table 1. Epoxidation of α-pinene catalyzed by different catalysts

Entry	Catalyst	Co content, wt %[a]	Conversion, %	Epoxide selec., %	TON
1	Na-MOR	—	2.9	95.1	—
2	$[Co(NH_3)_6]^{3+}$-MOR	3.0	97.8	95.2	192.0
3	$[Co(NH_3)_6]^{3+}$-Y	2.9	91.5	86.8	185.8
4	$[Co(NH_3)_6]^{3+}$-β	2.9	89.4	89.6	181.5
5	$[Co(NH_3)_6]^{3+}$-ZSM-5	2.8	77.7	90.6	163.5
6	$[Co(NH_3)_6]^{3+}$-MCM-22	2.8	84.5	78.8	177.8
7	$[Co(NH_3)_6]^{3+}$-13X	2.9	71.2	83.7	144.6
8	$[Co(NH_3)_6]Cl_3$/MOR[a]	10.0	85.5	85.5	15.1
9	$[Co(NH_3)_6]Cl_3/SiO_2$[a]	10.0	83.6	92.3	14.8
10	$[Co(NH_3)_6]Cl_3/TiO_2$[a]	10.0	31.1	82.6	5.5

Reaction conditions: α-pinene (3.0 mmol), initiator (CHP 0.3 mmol), DMF (10 g), catalyst (30 mg), 90°C, 5 h, 40 mL/min air.
[a] Catalyst: 100 mg.

ume, the actual exchange content of Co measured by ICP was 1.5–3.0%), there was a vigorously increase of α-pinene conversion from 77.4 to 97.8% with high selectivity of α-epoxypinane. But as the content of cobalt exchange continued to increase, the aggregation of active sites resulted in a slight decrease in the conversion of α-pinene.

Further investigation showed the significance of an appropriate solvent for the reaction (Fig. 8). The conversion of α-pinene ascended in the order of tert-butanol (0%) < DMA (2.1%) < THF (4.9%) < toluene (5%) < 1,4-dioxane (41.3%) < DMF (97.8%). This indicated that the trivalent cobalt might also form an active center state with DMF, which effectively activated oxygen molecules and facilitated the epoxidation reaction of α-pinene. Obviously, DMF was the optimal solvent for the target reaction.

Table 2 displayed the effect of different initiators on the reactions. It could be seen that $[Co(NH_3)_6]^{3+}$-MOR converted 36.3% of α-pinene without the addition of initiator (Entry 1). Compared with CHP and TBHP, the other initiators included H_2O_2, α-epoxypinane, and $Na_2S_2O_3$ were inefficient for the titled reaction under current experimental conditions. Once H_2O_2 was used in the epoxidation reaction, the conversion of α-pinene was only 28.2%, and the initiator

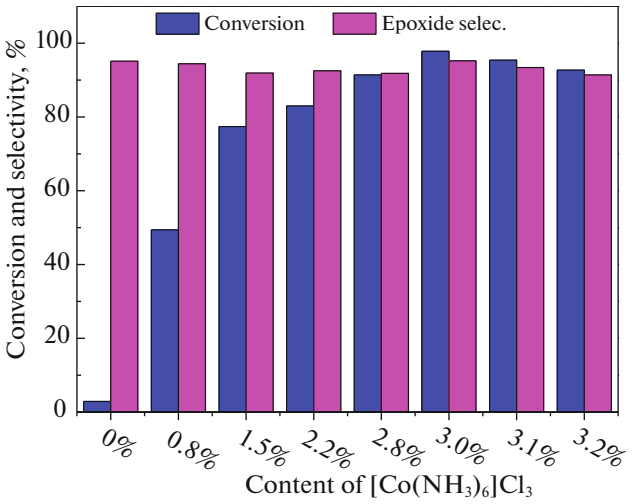

Fig. 7. Effect of $[Co(NH_3)_6]Cl_3$ content on the epoxidation. Reaction conditions: α-pinene (3.0 mmol), initiator (CHP 0.3 mmol), DMF (10 g), catalyst ($[Co(NH_3)_6]^{3+}$-MOR, 30 mg), 90°C, 5 h, 40 mL/min air.

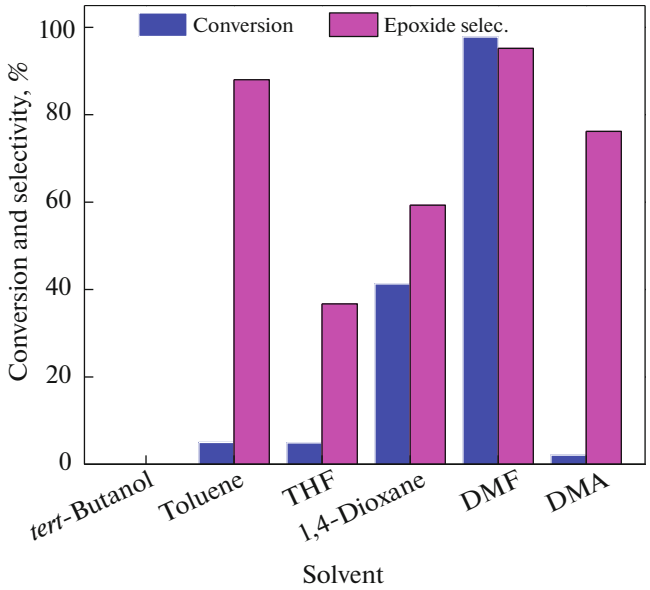

Fig. 8. Effect of solvent on the epoxidation reaction. Reaction conditions: α-pinene (3.0 mmol), initiator (CHP 0.3 mmol), solvent (10 g), catalyst (3%$[Co(NH_3)_6]^{3+}$-MOR, 30 mg), 90°C, 5 h, 40 mL/min air.

Table 2. Effect of initiators on the epoxidation of α-pinene

Entry	Catalyst	Initiator	Conversion, %	Epoxide selec., %
1	3%$[Co(NH_3)_6]^{3+}$-MOR	—	36.3	93.6
2		H_2O_2	28.2	88.8
3		α-Epoxypinane pinane	69.1	87.0
4		CHP	97.8	95.2
5		TBHP	96.1	92.3
6		$Na_2S_2O_3$[a]	49.4	87.4

Reaction conditions: α-pinene (3.0 mmol), initiator (CHP 0.3 mmol), DMF (10 g), catalyst (30 mg), 90°C, 5 h, 40 mL/min air.
[a] Initiator: 0.1 mmol.

$Na_2S_2O_3$ achieved 49.4% α-pinene conversion and approximately 87.4% selectivity of epoxide. When α-epoxypinane was used as the initiator, 69.1% conversion of α-pinene was acquired. As the organic peroxide TBHP was used as the reaction initiator, the pinene conversion increased rapidly to 96.1%, and the epoxide selectivity was 92.3%. However, once organic peroxide CHP was used as the reaction initiator, α-pinene reached the higher conversion of 97.8% and the higher epoxide selectivity of 95.2%.

Under the same reaction conditions, the amount of substrate had a certain effect on the epoxidation reaction, and the related reaction results were shown in Fig. 9. As 1 mmol of α-pinene was added to participate in the reaction, it achieved 100% α-pinene conversion. Continued to augment the α-pinene amount to 2 and 3 mmol, accordingly the conversion of α-pinene showed a slight decrease but still remained above 95%. While the amount of α-pinene was enlarged to 5 mmol, the conversion of α-pinene could maintain at 90%. But once the amount of α-pinene came up to 6 and 10 mmol, the conversion of α-pinene had a conspicuous decline (<80%), it might be due to the increase of α-pinene concentration and insufficient catalytic active center. Therefore, 3 mmol of α-pinene was considered as the optimal amount of substrate under other conditions.

Figure S5 described the consequence of the catalyst amount on the epoxidation reactions. When no catalyst existed, merely 8.7% of α-pinene was converted. And when the catalyst amount gradually increased from 10 to 30 mg, the α-pinene conversion speedily aggrandized from 73.5 to 97.8%, the selectivity of epoxide was maintained at about 95%. With further aggrandizing the catalyst to 200 mg, the α-pinene conversion and the α-epoxydecane selectivity decreased markedly. This was because as the catalyst amount increased, too many cobalt active sites aggregated, causing active site difficult to be contacted with, which led to a decrease in conversion. Meanwhile, more cobalt active sites also promoted the occurrence of some side reactions, leading to the drop of yield. This showed that excessive catalyst was ill-suited for the reaction. In summary, when 30 mg catalyst was added, the maximal yield of α-pinene was attained.

As can be seen in Fig. 10, the reaction temperature had a greater influence on the epoxidation reaction. Once raising the temperature from 60 to 90°C, the α-pinene conversion showed a sharp increase from 27.1 to 97.8% and the selectivity of α-epoxydecane showed a slight decrease, indicating that sufficient temperature was indispensable for the system. Along with the temperature increased to 95°C, the conversion of α-pinene showed a continuous increase, but the selectivity of α-pinene oxide was sharply decreased, possibly ascribed to the generation of some by-products. So keeping the temperature of the reaction system at 90°C was beneficial to the high efficiency and high selectivity of the reaction. Figure S6 explored the effect of reaction time on the results of the epoxidation reaction. With the reaction time increased, the conversion of α-pinene rapidly increased with the increase of reaction time from approximately 11.1% in 1 h to 36.4% in 2 h, and then

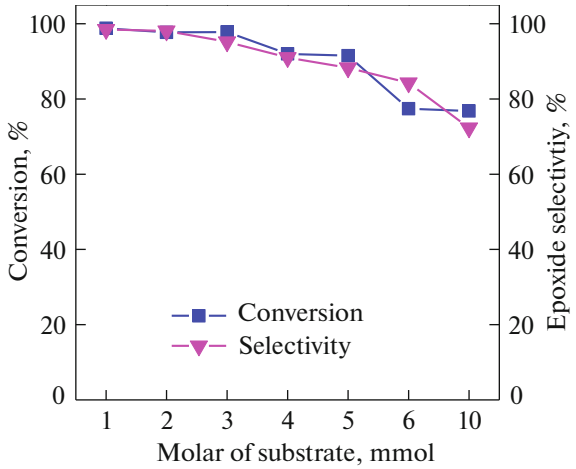

Fig. 9. Influence of the molar amount of substrate on the epoxidation reaction. Reaction conditions: α-pinene, initiator (CHP 0.3 mmol), DMF (10 g), catalyst (3%$[Co(NH_3)_6]^{3+}$-MOR, 30 mg), 90°C, 5 h, 40 mL/min air.

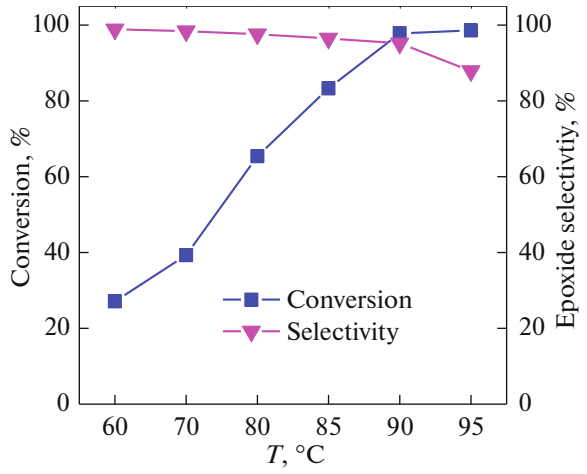

Fig. 10. Effect of reaction temperature on the epoxidation reaction. Reaction conditions: α-pinene (3.0 mmol), initiator (CHP 0.3 mmol), DMF (10 g), catalyst (3%$[Co(NH_3)_6]^{3+}$-MOR, 30 mg), 5 h, 40 mL/min air.

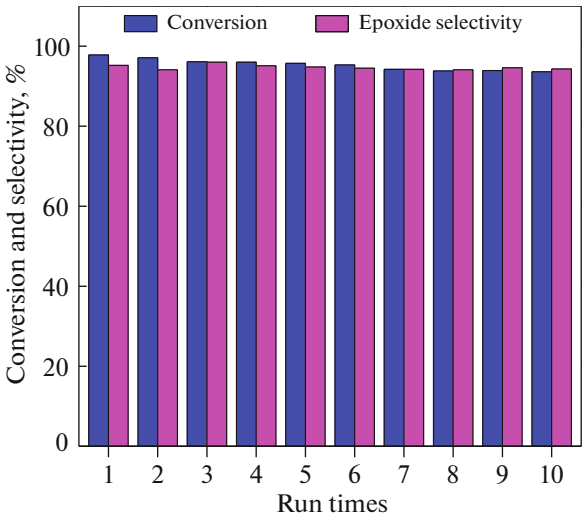

Fig. 11. The recycling results of 3%$[Co(NH_3)_6]^{3+}$-MOR catalyst. Reaction conditions: α-pinene (3.0 mmol), initiator (CHP 0.3 mmol), DMF (10 g), catalyst (3%$[Co(NH_3)_6]^{3+}$-MOR), 90°C, 5 h, 40 mL/min air.

to 85.8% in 3 h. When keeping increasing the reaction time to 4, 5, and 6 h, the conversion of olefin enhanced to 91.8, 97.8, and 99.5%, respectively. However, the selectivity of α-epoxydecane was in descending order with the increase of reaction time: 98.7% (1 h) > 98.1% (2 h) > 96.7% (4 h) > 95.2% (5 h) > 91.8% (6 h). Because the overall yield was considered as the main factor, the reaction time of 5 h was the optimal time for other reaction conditions.

The recycling experiments of $[Co(NH_3)_6]^{3+}$-MOR material for the epoxidation reaction were implemented. As was revealed in Fig. 11, even though the catalyst has been used ten times, the activity of catalyst sustained basically unaffected. After the epoxidation for α-pinene, the $[Co(NH_3)_6]^{3+}$-MOR material was recycled by filtration, then washed with ethanol, dried at 90°C and reused. Each of these reactions maintained nearly >95% conversion of α-pinene, and epoxide selectivity was stable at around 91%, which certified the recyclable stability of the $[Co(NH_3)_6]^{3+}$-MOR catalyst. The conversion of α-pinene in the subsequent several reactions decreased slightly, but the yield of α-epoxypinane also maintained above 88%. The reason for the slight decrease in yield might be the physical loss when recovering the catalyst.

The results of the kinetic experiment at different temperatures were shown in Fig. 12. As shown in Fig. 12a, the pseudo first-order model can be used to calculate the catalytic rate. It could express the kinetic equation for the reaction as $-\ln(C/C_0) = kt$, where C and C_0 were the α-pinene concentration at time t and the initial α-pinene concentration, k was the rate constant and t was the epoxidation reaction time. The k values for the epoxy reaction at 353, 363, and 368 K could be calculated from the slopes of these fitted lines in Fig. 12a, to be 0.4284, 0.6194, and 0.8429 h^{-1}, respectively. Therefore, the Arrhenius equation ($\ln k = \ln A - E_a/RT$, A was pre-exponential factor, T was reaction temperature, and R was the gas constant (8.314 J/(K mol)) could be applied to calculate the activation energy (E_a). The E_a value for the α-pinene epoxidation reaction could be calculated from the slope of the fitted line in Fig. 12b, and the calculated E_a value was 67.62 kJ/mol.

Under identical experimental conditions, the epoxidation reactions of six olefins were investigated (Fig. 13). For the epoxidation of α-pinene, approximately 97.8% of α-pinene was converted and there was 95.2% selectivity of α-epoxypinane. Meanwhile, the reactivity of α-methyl styrene and styrene were similar to that of α-pinene. However, the catalyst did not exhibit activity for linear olefins and macrocyclic olefins. In comparison, the conversion of six olefins decreased with the order of α-methyl styrene (98.5%) > α-pinene (97.8%) > styrene (95.5%) > cyclooctene (21.6%) > β-pinene (18.4%) > 4-vinyl-1-cyclohexene (9.8%); however, the epoxide selectivity decreased with the order of 4-vinyl-1-cyclohexene (100%) = cyclooctene (100%) > α-pinene (95.2%) > styrene (84.8%) > β-pinene (79.2%) > α-methyl styrene (78.1%).

CONCLUSIONS

In this work, we prepared a series of MOR supported Cobalt complex. $[Co(NH_3)_6]^{3+}$-MOR material was an efficient catalyst for olefin epoxidation with air and had excellent recycle stability. It can be recycled nine times, and the catalytic activity did not lose sig-

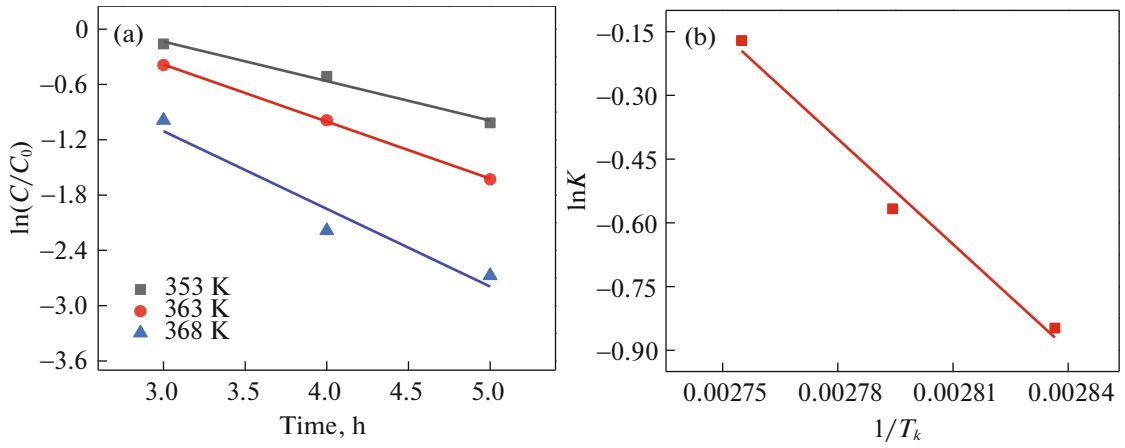

Fig. 12. (a) $\ln(C/C_0)$ versus reaction time and (b) Arrhenius plot of the α-pinene epoxidation at various temperatures.

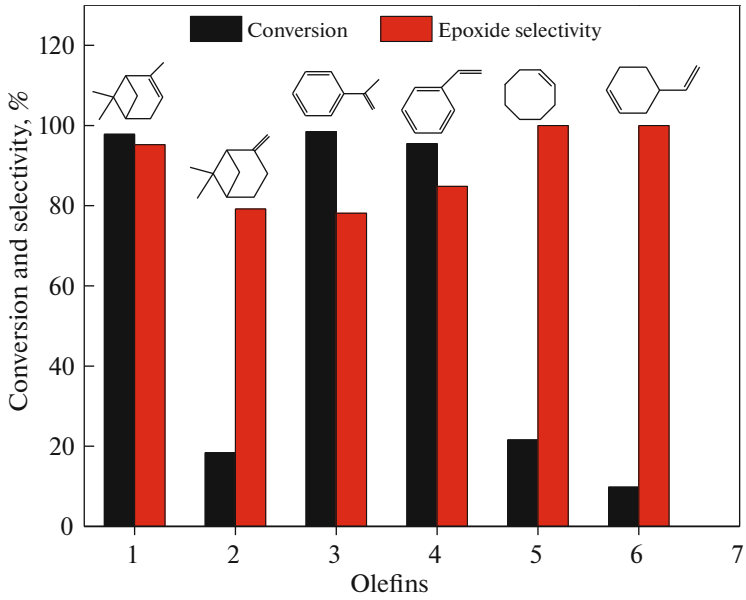

Fig. 13. Aerobic epoxidation of other olefins. Reaction conditions: α-pinene (3.0 mmol), initiator (CHP 0.3 mmol), DMF (10 g), catalyst (3%$[Co(NH_3)_6]^{3+}$-MOR, 30 mg), 90°C, 5 h, 40 mL/min air.

nificantly. The outstanding catalytic activity might be attributed to highly dispersed characteristics of $[Co(NH_3)_6]^{3+}$ ions exchanged onto the surface of MOR. The designed catalyst synthesis strategy was also applicable to other immobilized systems.

ACKNOWLEDGMENTS

The authors acknowledge the National Natural Science Foundation of China (22072038, U20A20122), the Hubei Student Innovation and Entrepreneurship Foundation of China (S202010512082, S201910512016), and Applied Basic Frontier Project of Wuhan Science and Technology Bureau (2019010701011415).

CONFLICT OF INTEREST

The authors declare that they have no conflicts of interest.

SUPPLEMENTARY INFORMATION

The online version contains supplementary material available at https://doi.org/10.1134/S0036024422120317.

REFERENCES

1. A. Blanckenberg and R. Malgas-Enus, Catal. Rev. **61**, 27 (2019).
2. T. Punniyamurthy, S. Velusamy, and J. Iqbal, Chem. Rev. **105**, 2329 (2005).

3. Q. H. Xia, H. Q. Ge, C. P. Ye, et al., Chem. Rev. **105**, 1603 (2005).
4. R. Neumann and M. Dahan, Nature (London, U.K.) **388**, 353 (1997).
5. E. Bosch and J. K. Kochi, J. Am. Chem. Soc. **118**, 1319 (1996).
6. Q. H. Martinez, M. E. Paez-Mozo, and O. F. Martinez, Top. Catal. **64**, 36 (2021).
7. S. Morales-de la Rosa, J. M. Campos-Martin, P. Terreros, and J. L. G. Fierro, Top. Catal. **58**, 325 (2015).
8. F. Cavani and J. H. Teles, ChemSusChem. **2**, 508 (2009).
9. D. H. Zhang, G. D. Li, J. X. Li, and J. S. Chen, Chem. Commun. **29**, 3414 (2008).
10. M. S. Batra, R. Dwivedi, and R. Prasad, Chem. Sel. **4**, 11636 (2019).
11. A. Ramanathan, R. Maheswari, and B. Subramaniam, Top. Catal. **58**, 314 (2015).
12. R. Jing, X. H. Lu, H. F. Zhang, et al., Chem. J. Chin. U. **40**, 528 (2019).
13. W. B. Ma, H. Y. Yuan, H. F. Wang, et al., ACS Catal. **8**, 4645 (2018).
14. P. Liu, H. Wang, Z. C. Feng, et al., J. Catal. **256**, 345 (2008).
15. U. Jameel, M. Q. Zhu, X. Z. Chen, and Z. F. Tong, Curr. Org. Chem. **21**, 2585 (2017).
16. Y. H. Tang, M. Yang, W. J. Dong, et al., Microporous Mesoporous Mater. **215**, 199 (2015).
17. J. Y. Liu, R. Meng, J. X. Li, et al., Appl. Catal. B **254**, 214 (2019).
18. J. Y. Liu, T. T. Chen, P. M. Jian, and L. X. Wang, Chin. J. Catal. **39**, 1942 (2018).
19. S. T. Wilson, B. M. Lok, C. A. Messina, et al., J. Am. Chem. Soc. **104**, 1146 (1982).
20. J. Z. Li, Y. X. Wei, G. Y. Liu, et al., Catal. Today **171**, 221 (2011).
21. M. Hong, S. G. Li, H. F. Funke, et al., Microporous Mesoporous Mater. **106**, 140 (2007).
22. Q. H. Tang, Y. Wang, J. Liang, et al., Chem. Commun. **4**, 440 (2004).
23. Q. H. Tang, Q. H. Zhang, H. L. Wu, and Y. Wang, J. Catal. **230**, 384 (2005).
24. T. Luts, R. Frank, W. Suprun, et al., J. Mol. Catal. A **273**, 250 (2007).
25. P. C. Bakala, E. Briot, L. Salles, and J. M. Bregeault, Appl. Catal. A **300**, 91 (2006).
26. B. Zhao and G. C. Wang, J. Phys. Chem. C **123**, 17273 (2019).
27. Y. M. Huang, Z. Liu, G. P. Gao, et al., ACS Catal. **7**, 4975 (2017).
28. G. Xu, H. Xia, X. H. Lu, et al., J. Mol. Catal. A **266**, 180 (2007).
29. B. Qi, X. H. Lu, S. Y. Fang, et al., J. Mol. Catal. A **334**, 44 (2011).
30. X. H. Lu, J. Lei, X. L. Wei. et al., J. Mol. Catal. A **400**, 71 (2015).
31. H. F. Zhang, J. He, X. H. Lu, L. Yang, C. L. Wang, F. F. Yue, and D. Zhou, New J. Chem. **44**, 17413 (2020).
32. B. Tang, X. H. Lu, D. Zhou, et al., Catal. Commun. **31**, 42 (2013).
33. D. Zhou, X. H. Lu, J. Xu, et al., Chem. Mater. **24**, 4160 (2012).
34. P. P. Tao, X. H. Lu, H. F. Zhang, et al., Mol. Catal. **463**, 8 (2019).
35. J. Bjerrum, J. P. McReynold, A. L. Oppegard, and R. W. Parry, Inorg. Synth. **2**, 216 (1946).